Mechatronics 71 (2020) 102420

Contents lists available at ScienceDirect

Mechatronics

journal homepage: www.elsevier.com/locate/mechatronics

Precise phase control of resonant MOEMS mirrors by comb-drive current feedback☆,☆☆

David Brunner *, Han Woong Yoo, Georg Schitter

TU Wien, Automation and Control Institute (ACIN), Gusshausstrasse 27–29, Vienna 1040, Austria

ARTICLE INFO

Keywords:
Comb-drive
Digital asynchronous phase locked loop (DAsPLL)
Micro-opto-electro-mechanical system (MOEMS)
Nonlinear systems
Precision control
Resonant scanning mirror

ABSTRACT

Accurate phase detection and control of nonlinear resonant micro-opto-electro-mechanical system (MOEMS) mirrors are crucial to achieve stable scanning motions and high resolution imaging as needed in precision applications. This paper proposes a precise phase detection method for an electrostatic actuated MOEMS mirror and a novel digital phase locked loop (PLL) that uses an asynchronous logic for high precision driving and immediate phase compensation, while the clock speed is kept low. The phase of the mirror is detected by an amplified current signal, generated by the movement of the comb drive electrodes, transimpedance amplifiers and a simple comparator circuit. An analysis of the proposed detection method reveals that the pointing uncertainty scales with the product of the driving voltage, the curvature of the comb drive capacitance and the angular velocity of the MOEMS mirror at the zero crossing. The developed fast start-up procedure brings the MOEMS mirror to its maximum amplitude within less than 100 ms with a minimum on required prior knowledge of the used device. The low optical pointing uncertainty of 0.3 mdeg obtained in closed loop operation, allows 19000 pixels with a precision of 10 sigma at a scanning frequency of 2 kHz.

1. Introduction

Resonant micro-opto-electro-mechanical system (MOEMS) mirrors receive much attention in high precision scanning and projection systems. They achieve large deflection angles at frequencies of several kilohertz, while the power consumption is low even at atmospheric pressure [1,2]. Further advantages are the excellent mechanical material properties and the ease of manufacturing with standard CMOS technology on a silicon wafer [3]. MOEMS mirrors have been studied and applied for several applications such as in compact displays [4], surface profilometry [5], optical coherence tomography [6] and automotive lidar [7]. Depending on the application requirements, their actuation principle can be electrostatic, electromagnetic, electrothermal or piezoelectric [1]. Among them, the electrostatic actuation using comb drives is the simplest to manufacture, as they can be made solely by structural patterning without additional processing steps.

In high precision scanning systems, accurate pixel synchronization to the mirror motion is critical for the image quality. For a targeted number of pixels, the maximum angular velocity defines the required accuracy of the pixel triggering signals. Therefore, the allowed pixel synchronization error scales inverse-proportionally with the mirror frequency. For example, to achieve a SVGA resolution (800 × 600) with a 40 Hz frame rate, a minimum fast axis scanning frequency of 37.3 kHz is required, resulting in a pixel duration at the center of 10.6 ns [8]. However a 50 Hz frame rate requires 47.1 kHz and has a pixel duration of only 8.4 ns.

In order to provide precise laser synchronization signals and to maintain the high amplitude MOEMS mirror oscillation, even if environmental conditions change, a phase locked loop (PLL) is applied [9]. Contrary to a conventional PLL application, where its output is synchronized to an externally applied reference signal, the PLL has to synchronize to the MOEMS mirror oscillation, which is in turn influenced by the PLL output. The stability of such a configuration for a nonlinear oscillator with a cubic stiffening spring is analyzed in [10], where the method of averaging is applied on the governing equation of motion. However MOEMS mirrors typically show additional nonlinearities such as the electrostatic actuation, which has a nonlinear voltage and mirror position dependency [11], making the analysis of the

☆ This work has been supported in part by the Austrian Research Promotion Agency (FFG) under the scope of the LiDcAR project (FFG project number 860819).
☆☆ This paper was recommended for publication by Associate Editor Tom Oomen.
* Corresponding author.
E-mail addresses: brunner@acin.tuwien.ac.at (D. Brunner), Yoo@acin.tuwien.ac.at (H.W. Yoo), schitter@acin.tuwien.ac.at (G. Schitter).

https://doi.org/10.1016/j.mechatronics.2020.102420
Received 29 January 2020; Received in revised form 19 June 2020; Accepted 23 August 2020
Available online 12 September 2020

dynamics and the proper PLL design more difficult.

In addition to a fast phase tracking capability of the PLL, also the pixel synchronization jitter caused by the phase detection noise is of interest. Various phase detection methods for MOEMS mirrors are proposed in literature, such as piezoresistive, piezoelectric, capacitive and optical sensing. Piezoresistive and piezoelectric sensing methods are reported by Grahmann et al. [12] and Baran et al. [13], which can provide continuous angle measurement by stress induced resistance or electric field changes, respectively. These methods are already used for closed loop control, achieving promising results [14,15], but require the deposition and doping of materials and therefore additional processing steps in the manufacturing of the scanning mirror. Furthermore, both methods suffer from a relatively strong temperature dependency, which has to be compensated by calibration.

The capacitive sensing method is common for MOEMS mirrors, which uses for example amplitude or frequency modulation of a high frequency carrier to extract the oscillation amplitude and phase information from the comb drive capacitance variation [16,17]. The advantage for electrostatic actuated MOEMS mirrors is that the same comb drives can be used for sensing and for actuation. However these modulation based methods are rather complicated and suffer from feed-through of the driving signal to the sensing circuitry. To reduce the feed-through, an approach with dedicated comb drives only for sensing is proposed in [18], which adds complexity to the design and therefore cost. Another capacitive method is using an external capacitor that integrates the displacement current generated by the mirror movement and evaluates the resulting voltage signal [19]. However the proposed method requires high clock speeds and a fast ADC if it is used for high frequency mirrors in the range of several kilohertz.

The optical detection method uses a laser diode and an optical detector on the backside of the MOEMS mirror for angle measurement. The system proposed in [9] uses simple photo diodes as detectors, which provide a signal when they are crossed by the laser beam and therefore encode the mirror oscillation in timing events. This method reports the lowest phase detection jitter in the literature so far, with a standard deviation of 12 ns for a mirror frequency of 23 kHz. However the design is more complex since additional optical components are required close to the MOEMS mirror.

The MOEMS mirror driving and pixel synchronization precision depends on both the phase detection capabilities as well as the PLL implementation. While analog PLLs [20] usually achieve high timing resolution, they consist of rather complicated circuitry and hardly allow complex control algorithms. On the other hand, digital PLLs [9,19] are rather easy to implement and provide many possibilities in control design. Furthermore, square wave driving signals with arbitrary duty cycle can be easily generated, which allows to reach higher mirror amplitudes compared to sine wave signals with the same maximum voltage [21]. However digital PLLs require high clock speeds to resolve timing signals with a high resolution.

The contribution of this paper is the detailed analysis and demonstration of a phase detection method using the comb drive displacement current, caused by the MOEMS mirror oscillation. The current signal shows a sharp zero crossing when the mirror passes the zero angle position and therefore a precise phase measurement can be provided by a comparator with a threshold at zero volt. For demonstration a digital asynchronous PLL (DAsPLL) is developed, with high precision phase tracking capabilities. This paper is an extension of the former publication [22], where the principle of the DAsPLL is proposed. The DAsPLL precisely detects and immediately compensates the phase error by switching off the MOEMS mirror driving signal with the comparator output asynchronously to the internal clock. At a quarter mirror period after a detected zero crossing, the driving signal is switched on again, resulting in a square wave driving signal with zero phase to the mirror oscillation. Since the presented method uses the same comb drives for actuation and for sensing, the MOEMS mirror design is simple and no additional components are required at the proximity of the mirror. Herein the analysis and verification are enhanced compared to the preliminary results in [22]. Additionally, a special learning mode allows a fast start-up of the MOEMS mirror and also a low re-lock time after sudden disturbances.

The paper is organized as follows. Section 2 describes the MOEMS mirror phase detection method and the dependencies of the achievable resolution is discussed. In Section 3 the used MOEMS mirror, the driving and sensing circuitry as well as the DAsPLL principle and the fast start-up method are described. Section 4 provides the experimental results of the fast start-up and the closed loop operation. In Section 5 the paper is concluded.

2. Phase detection of MOEMS mirror

Accurate phase detection is required to keep the pixel synchronization jitter low. In the following, the proposed phase detector is discussed, which uses the amplified displacement current, generated by the movement of the comb drive electrodes, with a sharp zero crossing when the mirror passes the zero angle position. The capacitance between the rotor and stator comb drive electrodes can be generally expressed as

$$C(\theta_\mathrm{m}) = C_0 + C_\Delta(\theta_\mathrm{m})\,, \tag{1}$$

where θ_m is the mirror rotation angle, C_0 is the comb drive capacitance at zero angle and $C_\Delta(\theta_\mathrm{m})$ is the variable capacitance with $C_\Delta(0) = 0\,\mathrm{F}$.

Besides the transient behavior at the edges of the square wave driving signal, the applied voltage V between the comb drive electrodes is constant, and the measured displacement current can be expressed as

$$I = V\,\frac{\mathrm{d}C(\theta_\mathrm{m})}{\mathrm{d}t} = V\,\frac{\mathrm{d}C_\Delta(\theta_\mathrm{m})}{\mathrm{d}\theta_\mathrm{m}}\,\frac{\mathrm{d}\theta_\mathrm{m}}{\mathrm{d}t}\,, \tag{2}$$

where $\frac{\mathrm{d}C_\Delta(\theta_\mathrm{m})}{\mathrm{d}\theta_\mathrm{m}}$ is a pure geometrical parameter and $\frac{\mathrm{d}\theta_\mathrm{m}}{\mathrm{d}t}$ is the angular velocity. The variable comb drive capacitance and its angular derivative are exemplary shown in Fig. 1, which are obtained by an actuated decay measurement [23]. The almost triangular shape of the capacitance is due to the changed overlap area A_ov of stator and rotor combs caused by the rotation as illustrated in Fig. 2 and also discussed in [24]. Hence, also other comb drive actuated resonant MOEMS mirror designs show capacitance curves of similar shape [19,21,24–26].

It follows that the displacement current provides a zero crossing when the mirror crosses the position with the maximum capacitance, i.e. the zero angle position. Using this property, the simplest implementation of a phase detector is a comparator with a threshold corresponding to zero current. As the MOEMS mirror has two zero crossings per period, this method provides one precise phase measurement in each mirror half period. The phase detection jitter is then defined by the steepness of the current at the zero crossing, which can be calculated by

$$\frac{\mathrm{d}I}{\mathrm{d}t} = V\left[\frac{\mathrm{d}^2C_\Delta(\theta_\mathrm{m})}{\mathrm{d}\theta_\mathrm{m}^2}\left(\frac{\mathrm{d}\theta_\mathrm{m}}{\mathrm{d}t}\right)^2 + \frac{\mathrm{d}C_\Delta(\theta_\mathrm{m})}{\mathrm{d}\theta_\mathrm{m}}\,\frac{\mathrm{d}^2\theta_\mathrm{m}}{\mathrm{d}t^2}\right]. \tag{3}$$

The second term in the square brackets is negligible at $\theta_\mathrm{m} = 0^\circ$ since

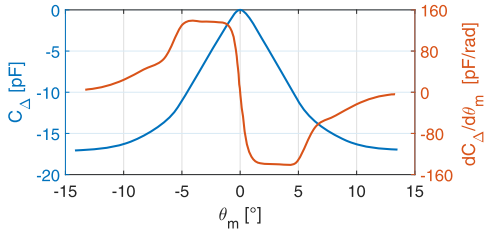

Fig. 1. Measured comb drive capacitance of the MOEMS mirror and its angular derivative. Since the capacitance is maximum at zero angle of the mirror, its derivative provides a sharp zero crossing.

Published version of the article: D. Brunner, H.W. Yoo, and G. Schitter, "Precise phase control of resonant MOEMS mirrors by comb-drive current feedback", *Mechatronics*, vol. 71, 102420, 2020. DOI: 10.1016/j.mechatronics.2020.102420

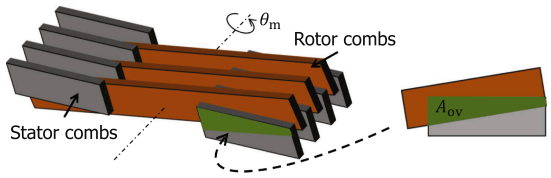

Fig. 2. Illustration of the overlap area A_{ov} dependency on the movement of the rotor combs.

the capacitance gradient and the inertial force are close to zero. The low inertial force can be shown by using the nonlinear parametric oscillator model given in [23] as the spring, the damping and the actuation torque are low at the zero crossing. Due to the symmetric design, the angular velocity is maximum at the zero crossing and is equal to the velocity amplitude $\dot{\Theta}_m$. Therefore, the steepness of the current at the zero crossing scales with the product of the applied voltage, the curvature of the comb drive capacitance at zero angle and the squared angular velocity amplitude, i.e.

$$\frac{dI}{dt}\Big|_{\theta_m=0^*} = V \frac{d^2 C_\Delta(\theta_m)}{d\theta_m^2}\Big|_{\theta_m=0^*} \dot{\Theta}_m^2 . \tag{4}$$

Eq. (4) can be used to analyze how a noise on the current signal affects the phase detection error Δt, i.e. the timing error between the actual zero crossing and the switching of the phase detection comparator. Herein the phase detection error is expressed in time, as due to the MOEMS mirror nonlinearities its trajectory is in general no single harmonic anymore. Assuming a constant additive Gaussian noise with a standard deviation σ_I on the current signal, the standard deviation of the phase detection error can be expressed as

$$\sigma_{\Delta t} = \frac{dt}{dI}\Big|_{\theta_m=0^*} \sigma_I = \left(V \frac{d^2 C_\Delta(\theta_m)}{d\theta_m^2}\Big|_{\theta_m=0^*} \dot{\Theta}_m^2 \right)^{-1} \sigma_I . \tag{5}$$

The inversion of (4) is well defined as long as the driving voltage at the zero crossing and the angular velocity amplitude are nonzero. Hence, the standard deviation scales inverse-proportionally with the squared mirror velocity. However, for faster mirrors the same pixel synchronization error Δt_{px} results in an increased optical pointing error $\Delta\theta_{opt}$, as

$$\Delta\theta_{opt} = 2 \frac{d\theta_m}{dt} \Delta t_{px} , \tag{6}$$

where the factor 2 comes from the optical leverage. In a PLL application, the pixel synchronization error depends on both the phase detection error as well as the PLL implementation.

In the following, the theoretical achievable resolution of a scanning system with the proposed phase detection method is analyzed. It is assumed that the laser shooting is not limited by any clock speed and the driving signal jitter has no considerable effect on the MOEMS mirror oscillation. Additionally, the PLL does not perform any filtering of the phase detection error, which is the worst case. According to (6) the maximum optical pointing error is where the angular velocity is the highest, i.e. $\dot{\Theta}_m$ at the zero crossing. There, the laser shot is triggered directly with the phase detection comparator switching and therefore the pixel synchronization error equals the phase detection error, i.e. $\Delta t_{px} = \Delta t$. Hence the worst optical pointing uncertainty σ_{opt} is given as

$$\sigma_{opt} = 2\,\dot{\Theta}_m\,\sigma_{\Delta t} = 2 \left(V \frac{d^2 C_\Delta(\theta_m)}{d\theta_m^2}\Big|_{\theta_m=0^*} \dot{\Theta}_m \right)^{-1} \sigma_I . \tag{7}$$

Eq. (7) shows how the minimum pixel size of the scanning system depends on the MOEMS mirror design parameters and the operation condition.

The pixel size d_{px} is given by the field of view (FoV) divided by the number of pixels N_{px}, i.e.

$$d_{px} = \frac{4\,\Theta_m}{N_{px}} . \tag{8}$$

Assuming a Gaussian distribution of the pointing error of a pixel defined by σ_{opt}, the probability that the pixel error is not within $\pm d_{px}/2$ can be calculated by

$$P_{out} = \mathrm{erfc}\left(\frac{d_{px}}{2\sqrt{2}\,\sigma_{opt}} \right) = \mathrm{erfc}\left(\frac{4\,\Theta_m}{N_{px}\,2\sqrt{2}\,\sigma_{opt}} \right) . \tag{9}$$

For high quality imaging, the pixel size should be much bigger than the worst optical uncertainty to keep the outlier probability low. In this investigation, the pixel size is chosen to be 10 σ_{opt}. Hence, (9) calculates to

$$P_{out} = \mathrm{erfc}\left(\frac{5}{\sqrt{2}} \right) = 5.73 \cdot 10^{-7} , \tag{10}$$

where the optical pointing error of the worst pixel results in 0.1 outliers per operation hour, assuming a 50 Hz frame rate. The number of pixels is then

$$N_{px} = \frac{4\,\Theta_m}{10\,\sigma_{opt}} . \tag{11}$$

Considering a phase detection method by using photo diodes, the laser crosses the diodes with higher speed for faster mirrors, leading to sharper edges of the sensing signal. Hence the phase detection standard deviation $\sigma_{\Delta t}$ scales inverse-proportionally with the mirror velocity. This theoretically results in a linear increase of N_{px} by the scanner amplitude but does not change with the scanning frequency as σ_{opt} is constant. However with the proposed current sensing based phase detection, the number of pixels is obtained by combining (7) and (11), as

$$N_{px} = \frac{1}{5} V \frac{d^2 C_\Delta(\theta_m)}{d\theta_m^2}\Big|_{\theta_m=0^*} \Theta_m \dot{\Theta}_m \frac{1}{\sigma_I} . \tag{12}$$

This shows that the scanning system resolution can be improved by increasing the product of the driving voltage, the curvature of the comb drive capacitance, the mirror amplitude and angular velocity, i.e. the frequency.

3. MOEMS mirror control design

Fig. 3 illustrates a schematic diagram of the proposed phase control loop and the evaluation setup. The DAsPLL is implemented in FPGA (Zedboard, Avnet, Phoenix, US) and operated at 100 MHz internal clock. The MOEMS mirror angle is measured using a position sensitive detector (PSD) and a continuous laser source [7]. A pulsed laser source and a CCD provide precise measurements of the optical pointing errors. The key elements of the phase control loop are the phase detector and the PLL, which define the overall system performance. In this section the MOEMS mirror, the driving and sensing circuitry and the working principle of the DAsPLL are described. Furthermore the DAsPLL is extended to achieve a fast start-up and a low re-lock time if sudden external influences disturb the system.

3.1. MOEMS mirror

Fig. 4 shows a picture of the used comb drive actuated resonant MOEMS mirror. The mirror is glued into a glass covered ceramic package with atmospheric pressure. Due to the driving voltage and angle dependent actuation torque of the comb drives, i.e.

$$\tau_{act} = \frac{1}{2} V(t)^2 \frac{dC_\Delta(\theta_m(t))}{d\theta_m} , \tag{13}$$

these MOEMS mirrors can be classified as parametrically excited

Published version of the article: D. Brunner, H.W. Yoo, and G. Schitter, "Precise phase control of resonant MOEMS mirrors by comb-drive current feedback", *Mechatronics*, vol. 71, 102420, 2020. DOI: 10.1016/j.mechatronics.2020.102420

systems [21,25,26]. One consequence is that the mirror can only oscillate at driving frequencies slightly above $2f_0/n$, where f_0 is the mirror natural frequency and n is a positive integer representing the order of the parametric resonance. The used mirror suspension by torsion bars and leaf springs improves the suppression of undesired modes and external shocks, but adds additional mechanical nonlinearities to the system. A modeling and identification method of the MOEMS mirror nonlinearities is described in [23]. Fig. 5 shows a steady state open loop frequency response of the MOEMS mirror where all transients are vanished. Herein the mirror frequency is calculated from adjacent zero crossings with the same direction. The driving signal has twice the mirror frequency to reach first-order parametric resonance, which provides the highest amplitudes. At increasing amplitudes the resonance frequency of the mirror also increases, which is called stiffening behavior, and is also shown in the backbone curve obtained by a decay measurement. Furthermore a bifurcation jump happens when the mirror changes its behavior from softening to stiffening. The phase delay provides the time difference between the negative edge of the driving signal and the zero crossing of the mirror, i.e. the driving voltage is switched off after the zero crossing of the mirror for positive delays. Hence, on the upper branch of the response curve, the zero crossing happens during the driving voltage is on. Some operation points, especially the high amplitudes, can hardly be directly reached in open loop when the mirror is at rest. The simplest but tedious way to reach the highest amplitude is to slowly sweep along the response curve.

In order to drive the MOEMS mirror with maximum energy injection for a given voltage, synchronized excitation is proposed by Schenk et al. [27]. At synchronized excitation, the voltage is switched on when the mirror angle is at its maximum and switched off at the zero crossing, which corresponds to the zero phase delay condition in Fig. 5, i.e. highest amplitude point. However the synchronized excitation is an operation point at the boundary to the fallback (red arrow in Fig. 5), where the amplitude drops rapidly, and can be hardly achieved and maintained in open loop.

3.2. Driving and sensing circuitry

Fig. 6 shows the used driving and sensing circuitry. The rotor potential of the mirror can be controlled by a single bit digital input D_{HVact}, i.e. generating square wave signals. The stator comb drive electrodes are connected to a trans-impedance amplifier (TIA), which provides the current signal V_{I}. As the sensing circuitry has a large impact on the system performance, two different settings are discussed in this paper. A low gain setting using a TIA gain G_{TIA} of 45.16 *V/mA* with a cut-off frequency at 270 kHz and an increased gain setting with a TIA gain of 93.28 *V/mA* with a resulting cut-off frequency at 148 kHz. If not explicitly mentioned, the low gain setting is used.

3.3. Digital asynchronous PLL (DAsPLL)

The injected comb drive energy per driving signal period can be expressed as

$$E_{\mathrm{C}} = \frac{V_{\mathrm{HV}}^2}{2}\left[C_\Delta\left(\theta_{\mathrm{m}}(t_{\mathrm{off}})\right) - C_\Delta\left(\theta_{\mathrm{m}}(t_{\mathrm{on}})\right)\right], \tag{14}$$

where t_{off} and t_{on} are the switching off and on time of the square wave driving signal, respectively. Therefore, the injected energy is only defined by these two time instances. In steady state, the dissipated energy is compensated by E_{C} and the corresponding switching times are the nominal values $\bar{t}_{\mathrm{off}}$ and $\bar{t}_{\mathrm{on}}$. The influence of the driving signal jitter can then be analyzed by the local time derivatives of (14). Using a Taylor approximation of up to the second order, the injected energy change can be expressed as

$$\begin{aligned}\Delta E_{\mathrm{C}} \approx \frac{V_{\mathrm{HV}}^2}{2}\Bigg[&\frac{\mathrm{d}C_\Delta\left(\theta_{\mathrm{m}}\left(\bar{t}_{\mathrm{off}}\right)\right)}{\mathrm{d}t}\Delta t_{\mathrm{off}} \\ &+\frac{\mathrm{d}^2C_\Delta\left(\theta_{\mathrm{m}}\left(\bar{t}_{\mathrm{off}}\right)\right)}{\mathrm{d}t^2}\frac{\Delta t_{\mathrm{off}}^2}{2} - \frac{\mathrm{d}C_\Delta\left(\theta_{\mathrm{m}}\left(\bar{t}_{\mathrm{on}}\right)\right)}{\mathrm{d}t}\Delta t_{\mathrm{on}} \\ &-\frac{\mathrm{d}^2C_\Delta\left(\theta_{\mathrm{m}}\left(\bar{t}_{\mathrm{on}}\right)\right)}{\mathrm{d}t^2}\frac{\Delta t_{\mathrm{on}}^2}{2}\Bigg],\end{aligned} \tag{15}$$

where Δt_{off} and Δt_{on} are the corresponding driving signal jitter. Using (2), (15) can be rewritten to

$$\begin{aligned}\Delta E_{\mathrm{C}} \approx \frac{V_{\mathrm{HV}}}{2}\Bigg[&I\left(\bar{t}_{\mathrm{off}}\right)\Delta t_{\mathrm{off}} + \frac{\mathrm{d}I\left(\bar{t}_{\mathrm{off}}\right)}{\mathrm{d}t}\frac{\Delta t_{\mathrm{off}}^2}{2} \\ &-I\left(\bar{t}_{\mathrm{on}}\right)\Delta t_{\mathrm{on}} - \frac{\mathrm{d}I\left(\bar{t}_{\mathrm{on}}\right)}{\mathrm{d}t}\frac{\Delta t_{\mathrm{on}}^2}{2}\Bigg].\end{aligned} \tag{16}$$

This shows the benefit of synchronized excitation, since the current at both switching times as well as the current gradient at the switching on time are almost zero as can be seen in Fig. 7, leading to a low disturbance of the mirror motion by the driving jitter. However the driving voltage should be accurately switched off at the zero crossing due to the high current gradient. The switching on time is more relaxed especially if the mirror is at a high amplitude, as the comb drive capacitance varies only marginally when the combs are fully disengaged. Hence, the DAsPLL is proposed for synchronized excitation and precise switching off of the driving voltage regardless of the internal clock.

The principle implementation of the DAsPLL is shown in Fig. 8. Two comparator signals D_{ZC} and D_{C1} are the inputs to the DAsPLL, which have negative edges at and slightly before the zero crossing of the mirror, respectively. The clock synchronized logic block measures the mirror period by adjacent zero crossing detections, using the comparator signals and provides a driving signal D_{HV} and a multiplexer control signal D_{MUX}. At a detected zero crossing, a counter is triggered that holds D_{HV} low for a quarter mirror period, which is derived from prior zero crossing detections. Subsequently D_{HV} gets high again, waiting for the next zero crossing of the mirror. Hence, a internal clock based square wave signal is generated on the output D_{HV}, which keeps synchronized excitation.

To switch the driving voltage off accurately at the zero crossing of the mirror without internal clock dependency, an asynchronous multiplexer MUX is implemented. The negative edge of the first comparator signal D_{C1} is used to switch the asynchronous multiplexer such that it connects the zero crossing comparator signal D_{ZC} directly to the driving output D_{HVact} of the DAsPLL. Therefore, if the current signal hits the zero crossing comparator threshold, the signal is forwarded to the driving circuitry and switches the voltage at the mirror off. After at least one clock cycle the multiplexer is switched back again and connects the synchronized driving signal D_{HV} to the driving output.

The threshold of the first comparator has to be properly chosen and depends on the obtained current signal, the measurement noise and the internal clock of the DAsPLL. A higher threshold requires a higher current signal, since it has to cross the threshold. A too low threshold, however, may increase the risk of false detections due to sensing noise, which may result in malfunctioning. Furthermore the time between the crossing of the first comparator and the zero crossing comparator has to be at least one clock cycle.

The DAsPLL immediately compensates the phase error with a high precision and stabilizes the MOEMS mirror with nonlinear dynamics.

Published version of the article: D. Brunner, H.W. Yoo, and G. Schitter, "Precise phase control of resonant MOEMS mirrors by comb-drive current feedback", *Mechatronics*, vol. 71, 102420, 2020. DOI: 10.1016/j.mechatronics.2020.102420

This is fundamentally different from conventional PLLs, which usually only adapt their frequency regarding the measured phase error [10]. The DAsPLL is directly locking on the mirror motion and spontaneously establishes synchronized excitation.

3.4. Fast start-up of MOEMS mirror

A comb drive actuated resonant MOEMS mirror is only able to start at specific driving conditions, given by the so called stability tongues [21,25]. In general it reveals that the frequency region where the MOEMS mirror can be started is limited and increases with the driving voltage and also depends on the duty cycle. In order to achieve a fast and reliable start-up of the MOEMS mirror, the mirror behavior has to be either predictable or the control loop has to be closed as soon as possible. Due to the uncertain start of the oscillation as well as process variations and environmental influences, the mirror may be hardly predictable at the start-up. Fig. 9 shows how the MOEMS mirror starts to oscillate when a constant driving frequency f_{dr} is applied according to first-order parametric resonance. The observed beating at the beginning is because the mirror frequency and amplitude vary due to its nonlinear dynamics, as can be seen in Fig. 10 until it converges to a steady state oscillation on the lower branch of the response curve.

In case of current sensing based phase detection, the zero crossing is required to happen during the driving voltage is on, corresponding to a positive phase delay in Fig. 5. However the stable point in Fig. 10 has negative phase delay, meaning that the zero crossing is not detectable. Therefore, the driving frequency is usually slowly swept down in order to reach the bifurcation jump and to obtain a positive phase. The method presented in [28] achieves the bifurcation jump very fast by first applying a driving frequency where the mirror is able to start and after a specific time switching directly to the bifurcation frequency. As this is still an open loop method and the bifurcation frequency has to be known, this method may not be reliable enough as environmental conditions influence the bifurcation location. A faster and more reliable approach is to close the control loop already during the transient beating of an open loop start and run the mirror to the maximum amplitude. The proposed method is shown in Fig. 11. Once a valid zero crossing of the current signal is detected, i.e. both comparator thresholds are crossed in the correct order and successively in time, the learning mode is started. During the learning mode the voltage is constantly on and the DAsPLL measures the mirror period by successive zero crossings. After enough valid detections, the DAsPLL switches to the closed loop mode and runs the mirror to the maximum amplitude, by keeping zero phase delay. Except the initial open loop start and the learning mode, this method represents the fastest possible start-up for a given maximum driving voltage. Furthermore the proposed method does not require any knowledge about the MOEMS mirror but only a frequency band where the mirror can be started. The square wave signal of the open loop start does not have to be a single frequency but can be mixed frequencies or a chirp in order to minimize the required prior knowledge about the MOEMS mirror.

The learning mode is also applicable to minimize the re-lock time after environmental influences affected the MOEMS mirror or the sensing, such as mechanical shocks or strong electromagnetic interference. If unusual signals are obtained, the DAsPLL returns to the learning mode and tries to synchronize on the mirror movement again.

4. Experimental results

In this section, experimental results of the proposed fast start-up method and the achieved pointing uncertainty are discussed.

4.1. Verification of MOEMS mirror fast start-up

Fig. 12 shows the proposed fast start-up procedure, where the phase control loop is closed already about 20 ms after the begin of actuation. In closed loop, the mirror oscillation is precisely tracked for maximum energy injection such that the mirror is run to the highest amplitude as fast and reliable as possible. The MOEMS mirror amplitude over frequency behavior is shown in Fig. 13 for three different initial open loop driving frequencies f_{dr}. At the first two datasets, the initial driving frequency is twice the mirror frequency corresponding to the first-order parametric resonance. The third dataset shows the proposed method at an initial start at the second-order parametric resonance, where the driving frequency is equal to the mirror frequency. After the learning mode, the response is almost the same for all initial start frequencies and the MOEMS mirror is run to maximum amplitude in the first-order parametric resonance by keeping zero phase delay. The sudden jumps to higher frequencies and back are due to the additional electrostatic stiffness caused by the comb drives during the learning mode. By the proposed start-up method the mirror can be run to 99.9% of the final amplitude within less than 100 ms depending on the chosen initial driving condition. This results show that each comb drive actuated resonant MOEMS mirror can be automatically run to its maximum amplitude by using the proposed fast start-up method, once it reaches a sufficient high current signal for a valid zero crossing detection.

4.2. Pointing uncertainty measurement

As the DAsPLL locks on the mirror movement and establishes synchronized excitation, the only remaining input to the system is the driving voltage V_{HV} and therefore defines the reached mirror amplitude. Fig. 14 shows the obtained steady state amplitude over driving voltage behavior.

In order to analyze the achieved optical resolution by the proposed phase detection method and control structure, a pulsed laser is triggered directly with the zero crossing signal asynchronously to the internal FPGA clock. By this, the pointing uncertainty of the DAsPLL at the zero crossing of the mirror can be measured by a CCD. The experimental setup is illustrated in Fig. 15. In order to obtain only a single shot in each frame, the exposure time is set to less than the mirror period. A video is captured for each amplitude point and analyzed regarding the standard deviation and the center displacement of the captured spots. For highly reliable detection of the spot movement on the CCD, the first captured frame in a video serves as a reference and is cross-correlated with the other frames. The large distance D between the MOEMS mirror and the CCD allows an angular resolution of 0.68 mdeg optically per pixel on the CCD. In order to achieve sub-pixel resolution, a Gaussian function is fitted to the result of the cross-correlation around the maximum point as can be seen in Fig. 16. As the used MOEMS mirror has only one oscillation axis, fitting is necessary only along the X axis of the CCD. The optical pointing error can be calculated by

$$\Delta\theta_{opt} = \tan^{-1}\left(\frac{\Delta r_{CCD}}{D}\right), \tag{17}$$

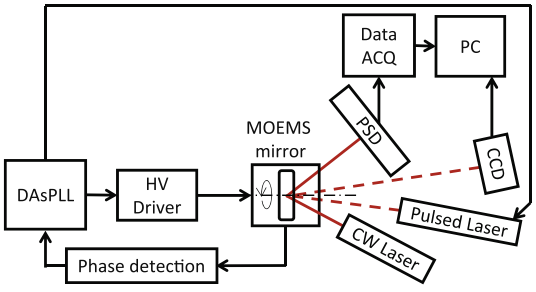

Fig. 3. Schematic diagram of the evaluation setup and the phase control loop. The mirror angle is measured by a PSD and a CCD provides a high resolution measurement of the pixel synchronization error.

Published version of the article: D. Brunner, H.W. Yoo, and G. Schitter, "Precise phase control of resonant MOEMS mirrors by comb-drive current feedback", *Mechatronics*, vol. 71, 102420, 2020. DOI: 10.1016/j.mechatronics.2020.102420

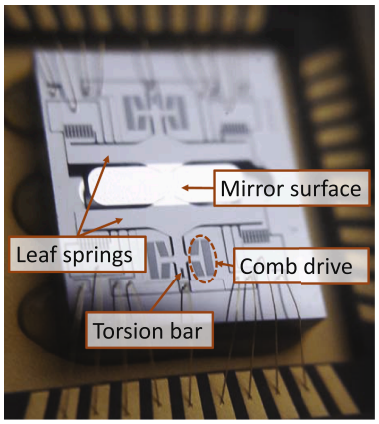

Fig. 4. Picture of the used comb drive actuated resonant MOEMS mirror in a glass covered ceramic package. The combined suspension with leaf springs and torsion bars prevents undesired modes while adding mechanical nonlinearities. The mirror is actuated by four identical and symmetrically placed comb drives.

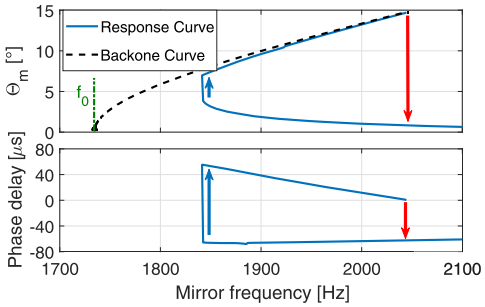

Fig. 5. Measured open loop frequency response of the used MOEMS mirror at 75 V actuation with 50% duty cycle. The blue upward arrow indicates a bifurcation point where an amplitude jump occurs. The amplitude further increases with increasing frequency until the fallback indicated by a red downward arrow. The backbone curve shows the pure mechanical behavior of the mirror and its natural frequency f_0 obtained by a decay measurement. The phase delay (bottom) provides the time difference between the negative edge of the driving signal and the zero crossing of the mirror. (For interpretation of the references to colour in this figure legend, the reader is referred to the web version of this article.)

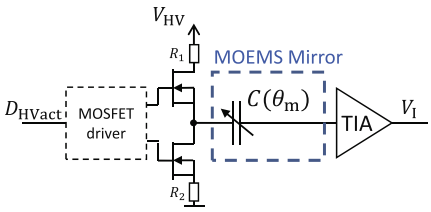

Fig. 6. Driving and sensing circuitry for MOEMS mirror. The single bit digitally controlled driving circuit switches the MOEMS mirror rotor potential between V_{HV} and ground. The current collected by the stator electrodes is converted to a voltage V_I by a TIA, which is used for phase detection.

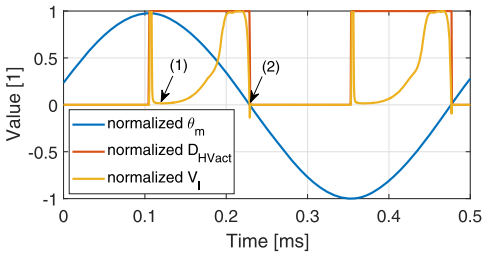

Fig. 7. Measured signals at synchronized excitation (V_{HV} = 72.5 V). The negative edge of the digital driving signal D_{HVact} coincides with the zero crossing of the current signal V_I and with the zero crossing of the mirror. As indicated by (2) the switching off current is low but with a high gradient. The current at the switching on is shown by (1) which is almost zero with a low gradient.The sharp peak before (1) is due to switching on the driving voltage and does not represent a comb drive capacitance change.

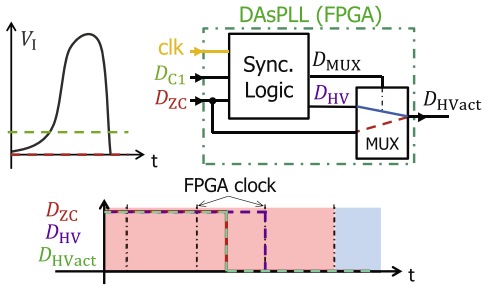

Fig. 8. Operation principle of the DAsPLL. (top-left) Illustration of a current signal V_I with comparator threshold values given by dashed lines. (top-right) DAsPLL scheme comprising a clock synchronized logic and an asynchronous multiplexer (MUX). The multiplexer is controlled by the synchronized logic and connects the driving output D_{HVact} directly to the zero crossing comparator signal D_{ZC} if a negative edge is detected on D_{C1}. (bottom) Asynchronous switching of the driving signal D_{HVact} without internal clock dependency.

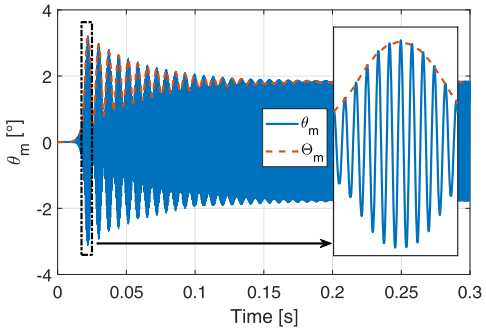

Fig. 9. Measured open loop start of the MOEMS mirror with constant driving frequency (f_{dr} = 3800 Hz, V_{HV} = 72.5 V). The mirror amplitude increases rapidly and starts beating until about 0.3 s after the actuation started.

where Δr_{CCD} is the relative spot movement on the CCD regarding the reference position, in meter.

Fig. 17 shows the obtained amplitude dependent center displacement, i.e. the mean value of $\Delta\theta_{opt}$, relative to the lowest amplitude case. This may be caused by three effects, the finite but constant time delay of

Published version of the article: D. Brunner, H.W. Yoo, and G. Schitter, "Precise phase control of resonant MOEMS mirrors by comb-drive current feedback", *Mechatronics*, vol. 71, 102420, 2020. DOI: 10.1016/j.mechatronics.2020.102420

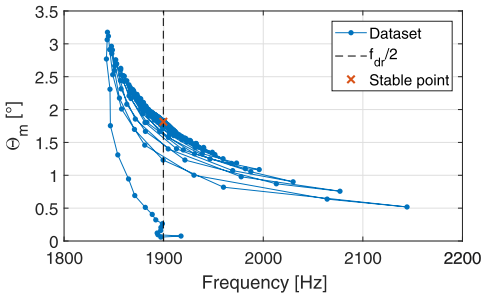

Fig. 10. Measured amplitude and frequency at an open loop start of the MOEMS mirror (V_{HV} = 72.5 V) with constant driving frequency f_{dr}.

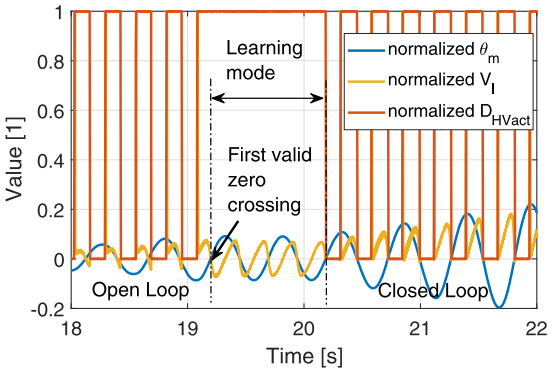

Fig. 11. Fast start-up method of MOEMS mirror using current sensing based phase detection. The MOEMS mirror is started in open loop (f_{dr} = 3800 Hz, V_{HV} = 72.5 V) until a first valid zero crossing is detected in the current signal. After the learning mode, where the mirror frequency is measured, the loop is closed and the MOEMS mirror is run to maximum amplitude.

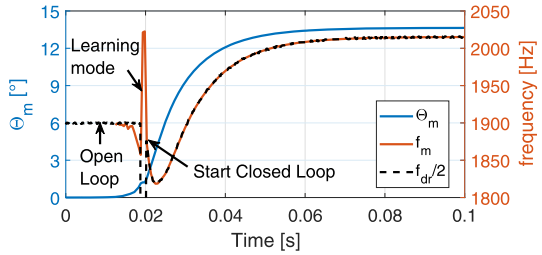

Fig. 12. Measured fast start-up using the proposed method (V_{HV} = 72.5 V). The phase control loop is closed already ~20 ms after the begin of actuation and 99.9% of the final amplitude is reached at 88.9 ms.

the pulsed laser, possible parasitic modes of the mirror and the band limitation of the current sensing circuitry, which delays the detected zero crossing. However in an application, this effect can be calibrated and therefore represents no restriction.

The asynchronous laser triggering results in a Gaussian shaped histogram of the optical pointing error as shown in Fig. 18. This jitter originates from a white noise source given by the current sensing circuitry and therefore directly reflects the phase detection error. The achievable optical resolution by the FPGA clock of 10 ns would be ~2 mdeg at the lowest and ~3.5 mdeg at the highest amplitude and

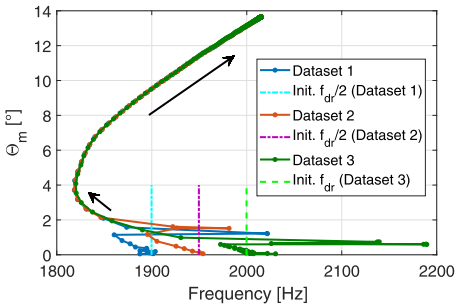

Fig. 13. MOEMS mirror amplitude over frequency behavior at the proposed fast start-up method (V_{HV} = 72.5 V). Datasets one and two initially start in first-order parametric resonance whereas the third dataset starts in second-order parametric resonance.

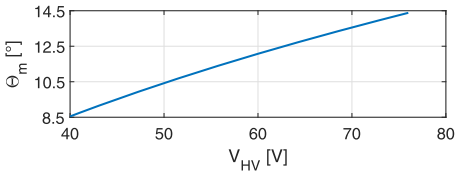

Fig. 14. Mechanical amplitude of the MOEMS mirror over applied driving voltage, when it is operated by the DAsPLL.

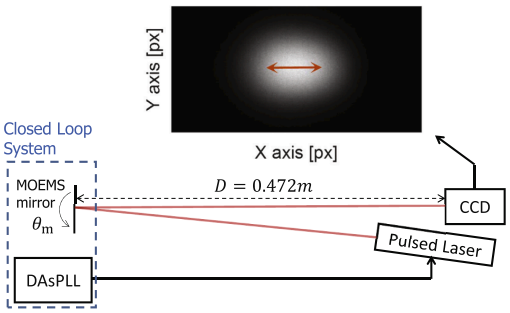

Fig. 15. Zoomed schematic of the evaluation setup in Fig. 3 and a CCD frame example. The DAsPLL asynchronously triggers the pulsed laser source with the phase detection signal, i.e. at the zero crossing of the mirror. The reflected beam directly hits the CCD chip and the optical uncertainty can be measured by analyzing the frames containing single shots. The direction of the spot movement due to pointing errors is indicated by a red double arrow. (For interpretation of the references to colour in this figure legend, the reader is referred to the web version of this article.)

would therefore show a distorted histogram. In Fig. 19 the obtained standard deviation of the pointing error is shown for the two different gain settings of the current sensing circuitry (see Section 3.2). In order to compare the results to the theoretical model given by (7) the model

$$\hat{\sigma}_{opt} = K_0 \left(V_{HV}\, \dot{\Theta}_m \right)^{-1}, \tag{18}$$

is fitted to the data where K_0 is the fitting constant and $\dot{\Theta}_m$ is measured by the PSD. Hence, the parameter K_0 represents twice the ratio of the standard deviation of the current signal noise to the comb drive capacitance curvature at zero angle, which are hard to measure accurately.

Published version of the article: D. Brunner, H.W. Yoo, and G. Schitter, "Precise phase control of resonant MOEMS mirrors by comb-drive current feedback", *Mechatronics*, vol. 71, 102420, 2020. DOI: 10.1016/j.mechatronics.2020.102420

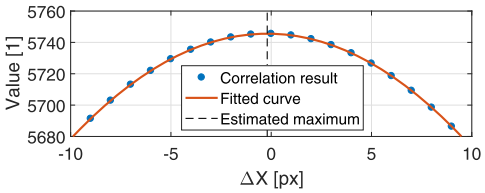

Fig. 16. Cross-correlation result of a CCD frame with the reference frame and a Gaussian fit. The fitting provides sub-pixel resolution with an estimated relative maximum shift of -0.2 px in this example.

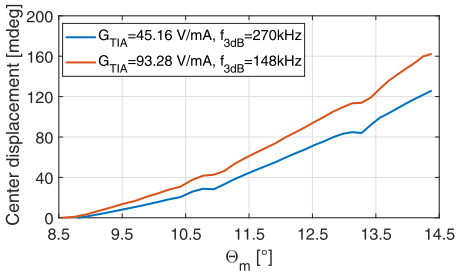

Fig. 17. Amplitude dependent center displacement measured by the CCD. The measurements are made with a high and a low gain setting of the current sensing circuitry. Due to the difference in bandwidth of the two settings, the CCD had to be manually moved between both measurements. Therefore the zero reference at low amplitudes are not the same for both measurements.

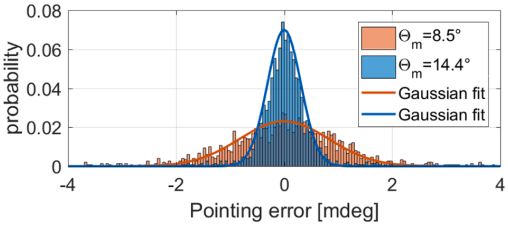

Fig. 18. Histogram of the measured optical pointing error at lowest and highest amplitude and their Gaussian fits. The datasets include 1500 measured single shot frames.

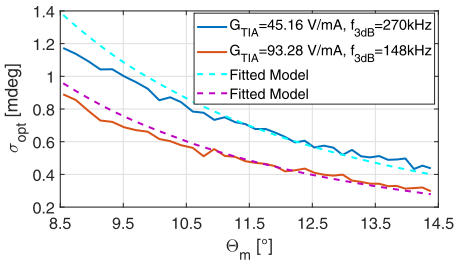

Fig. 19. Standard deviation of optical pointing error over mirror amplitude and theoretical fits using (18). The measurements are made with a high and a low bandwidth setting of the current sensing circuitry. The results show that for such small errors, the used bandwidth, drifts and also parasitic modes of the MOEMS mirror may affect the current gradient at the zero crossing.

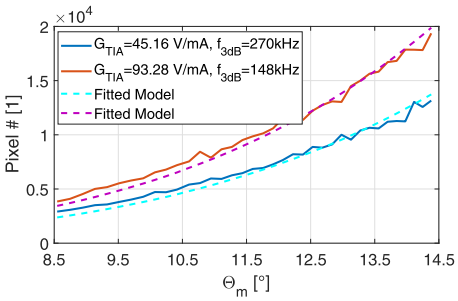

Fig. 20. Number of possible pixels using (11) and the fitted theoretical model given by (12). The data shows the expected disproportional increase of resolution by amplitude. The maximum achieved resolution is ~19000 pixels with a precision of 10 sigma.

The theoretical model and the measurements show good agreement in general. The small discrepancies can have several reasons as the obtained standard deviations are rather small. First, the MOEMS mirror is only phase controlled, so environmental fluctuations or the jitter of the driving voltage switching may cause errors due to the amplitude dependent center displacement. Furthermore the mirror has also parasitic modes that may cause a distortion of the current signal at the zero crossing. The bandwidth of the sensing circuitry also influences the results. If the gain is increased, the bandwidth is reduced and therefore also the current signal noise given by σ_I is decreased as well. Following this, the pointing uncertainty in Fig. 19 at the same operation amplitudes should be at least improved by a factor of ~ 2 as given by the ratio of the used TIA gains, but actually only achieves 1.46. This shows that the bandwidth may not be sufficient to accurately represent the actual current signal and distorts the current gradient at the zero crossing. Therefore, a further increase of the TIA gain may not improve the system performance significantly as the current gradient gets flattened due to a decreased bandwidth. Furthermore, it has to be considered that a low bandwidth causes a delay between the actual and the detected zero crossing, leading to a late switching off of the driving voltage by the DAsPLL. The minimum achieved optical standard deviation is 0.3 mdeg at a mirror amplitude of 14.38° and a scanning frequency of 2032 Hz corresponding to a phase detection standard deviation of only 0.84 ns.

Finally Fig. 20 shows the obtained possible number of pixels calculated by (11) with a precision of 10 sigma. The theoretical model (12) is fitted to the data and shows the expected disproportional increase of resolution. The maximum resolution achieved has about 19000 pixels at a FoV of 57.52°. The phase detection method based on photo diodes presented in [9] for a MOEMS mirror with about eleven times higher scanning frequency and a similar FoV of 40° would only achieve about 230 pixels with a precision of 10 sigma. Thus the phase detection errors have to be averaged to obtain a higher resolution, which makes the PLL more complex and slow. The model in (12) reveals that the current sensing based phase detection method would achieve even better performance if the scanning frequency is increased.

In summary it is shown that the developed DAsPLL using current sensing based phase detection is able to start and precisely operate comb drive actuated resonant MOEMS mirrors. The phase detection method does not require any additional component at the mirror or a complex circuitry and outperforms conventional photo diode based phase detection.

5. Conclusion

In this paper a simple high precision driving and fast tracking DAsPLL for comb drive actuated resonant MOEMS mirrors is proposed, utilizing a current sensing based phase detection and asynchronous

Published version of the article: D. Brunner, H.W. Yoo, and G. Schitter, "Precise phase control of resonant MOEMS mirrors by comb-drive current feedback", *Mechatronics*, vol. 71, 102420, 2020. DOI: 10.1016/j.mechatronics.2020.102420

logic. The phase of the mirror is measured by simple comparators, which detect the sharp zero crossing of the displacement current when the mirror crosses zero angle. The DAsPLL is implemented in a FPGA and consists of a synchronized logic and an asynchronous multiplexer, which are used to precisely operate the mirror in synchronized excitation. A learning mode of the DAsPLL allows a fast start-up and a low re-lock time while requiring only a minimum prior knowledge about possible start frequencies of the MOEMS mirror. Experimental results show the superior performance of the developed system, achieving a start-up time of less than 100 ms and an optical pointing uncertainty of 0.3 mdeg at a field of view of 57.52° with a scanning frequency of about 2 kHz. This allows 19000 pixels with a precision of 10 sigma, where one pixel delivers erroneous data only 0.1 times per operation hour, assuming a 50 Hz frame rate.

The provided analysis of the achievable number of pixels shows that the proposed sensing method carries the potential for high precision and high speed scanning control of MOEMS mirrors oscillating with tens of kilohertz.

CRediT authorship contribution statement

David Brunner: Conceptualization, Methodology, Software, Validation, Formal analysis, Investigation, Writing - original draft, Visualization. **Han Woong Yoo:** Conceptualization, Methodology, Writing - review & editing, Visualization, Supervision. **Georg Schitter:** Conceptualization, Writing - review & editing, Supervision, Project administration, Resources.

Declaration of Competing Interest

The authors declare that they have no known competing financial interests or personal relationships that could have appeared to influence the work reported in this paper.

References

[1] Holmström STS, Baran U, Urey H. MEMS laser scanners: a review. J Microelectromech Syst 2014;23(2):259–75.
[2] Nabholz U, Heinzelmann W, Mehner JE, Degenfeld-Schonburg P. Amplitude- and gas pressure-dependent nonlinear damping of high-q oscillatory MEMS micro mirrors. J Microelectromech Syst 2018;27(3):383–91.
[3] Petersen KE. Silicon as a mechanical material. Proc IEEE 1982;70(5):420–57.
[4] Liao C, Tsai J. The evolution of MEMS displays. IEEE Trans Ind Electron 2009;56 (4):1057–65.
[5] Yoshizawa T, Wakayama T, Takano H. Applications of a MEMS scanner to profile measurement. Proc. SPIE 6762. 2007. p. 89–93.
[6] Xie H, Fedder G, Pan Y. MEMS-based endoscopic optical coherence tomography. Proc. SPIE 5721. 2005. p. 81–92.
[7] Yoo HW, Druml N, Brunner D, Schwarzl C, Thurner T, Hennecke M, et al. MEMS-based lidar for autonomous driving. e & i Elektrotechnik und Informationstechnik 2018;135(6):408–15.
[8] Scholles M, Bräuer A, Frommhagen K, Gerwig C, Lakner H, Schenk H, et al. Ultra compact laser projection systems based on two-dimensional resonant micro scanning mirrors. Proc. SPIE 6466. 2007. p. 94–105.
[9] Tortschanoff A, Lenzhofer M, Frank A, Wildenhain M, Sandner T, Schenk H, et al. Position encoding and phase control of resonant MOEMS mirrors. Sens Actuators, A 2010;162(2):235–40.
[10] Fan M, Clark M, Feng Z. Implementation and stability study of phase-locked-loop nonlinear dynamic measurement systems. Commun Nonlinear Sci 2007;12(7): 1302–15.
[11] Pengwang E, Rabenorosoa K, Rakotondrabe M, Andreff N. Scanning micromirror platform based on MEMS technology for medical application. Micromachines 2016;7(2).
[12] Grahmann J, Graßhoff T, Conrad H, Sandner T, Schenk H. Integrated piezoresistive position detection for electrostatic driven micro scanning mirrors. Proc. SPIE 7930. 2011. p. 260–7.
[13] Baran U, Brown D, Holmstrom S, Balma D, Davis WO, Muralt P, et al. Resonant PZT MEMS scanner for high-resolution displays. J Microelectromech Syst 2012;21(6): 1303–10.
[14] Grahmann J, Dreyhaupt A, Drabe C, Schroedter R, Kamenz J, Sandner T. MEMS-mirror based trajectory resolution and precision enabled by two different piezoresistive sensor technologies. Proc. SPIE 9760. 2016. p. 20–30.
[15] Gu-Stoppel S, Giese T, Quenzer H-J, Hofmann U, Benecke W. PZT-actuated and -sensed resonant micromirrors with large scan angles applying mechanical leverage amplification for biaxial scanning. Micromachines 2017;8(7).
[16] Chemmanda LJ, Jianrong CC, Singh RP, Roterman Y. ASIC front-end for sensing MEMS-mirror position. 2014 International symposium on integrated circuits (ISIC). 2014. p. 396–9.
[17] Hung AC-L, Lai HY-H, Lin T-W, Fu S-G, Lu MS-C. An electrostatically driven 2D micro-scanning mirror with capacitive sensing for projection display. Sens Actuators, A 2015;222:122–9.
[18] Hofmann U, Janes J, Quenzer H. High-Q MEMS resonators for laser beam scanning displays. Micromachines (Basel) 2012;3:509–28.
[19] Roscher K-U, Fakesch U, Schenk H, Lakner HK, Schlebusch D. Driver ASIC for synchronized excitation of resonant micromirrors. Proc. SPIE 4985. 2003. p. 121–30.
[20] Li H-C, Tseng S-H, Huang P-C, Lu MS-C. Study of CMOS micromachined self-oscillating loop utilizing a phase-locked loop-driving circuit. J Micromech Microeng 2012;22(5):055024.
[21] Shahid W, Qiu Z, Duan X, Li H, Wang TD, Oldham KR. Modeling and simulation of a parametrically resonant micromirror with duty-cycled excitation. J Microelectromech Syst 2014;23(6):1440–53.
[22] Brunner D, Yoo HW, Schitter G. Digital asynchronous phase locked loop for precision control of MOEMS scanning mirror. IFAC-PapersOnLine 2019;52(15): 43–8.
[23] Brunner D, Yoo HW, Thurner T, Schitter G. Data based modelling and identification of nonlinear SDOF MOEMS mirror. Proc. SPIE 10931. 2019. p. 269–78.
[24] Izawa T, Sasaki T, Hane K. Scanning micro-mirror with an electrostatic spring for compensation of hard-spring nonlinearity. Micromachines 2017;8(8).
[25] Ataman C, Urey H. Modeling and characterization of comb-actuated resonant microscanners. J Micromech Microeng 2005;16(1):9–16.
[26] Frangi A, Guerrieri A, Carminati R, Mendicino G. Parametric resonance in electrostatically actuated micromirrors. IEEE Trans Ind Electron 2017;64(2): 1544–51.
[27] Schenk H, Durr P, Haase T, Kunze D, Sobe U, Lakner H, et al. Large deflection micromechanical scanning mirrors for linear scans and pattern generation. IEEE J Sel Top Quant 2000;6(5):715–22.
[28] Strasser A, Stelzer P, Steger C, Druml N. Speed-up of MEMS mirror's transient start-up procedure. IEEE Sens Appl Symp 2019:1–5.

David Brunner is PhD student at the Automation and Control Institute (ACIN) of TU Wien. He received his MSc. degree in Energy Systems and Automation Technology from TU Wien, Austria, in 2017. His primary research interests include advanced identification and control concepts, high performance mechatronic systems and system integration.

Han Woong Yoo is a postdoctoral researcher in Advanced Mechatronic Systems at the Automation and Control Institute (ACIN) of TU Wien. He received BS from Yonsei University and MS in Electrical Engineering from Seoul National University in 2007. Afterwards, he worked in Samsung Advanced Institute of Technology (SAIT) and Samsung Electronics co. LTD, semiconductor business for low power digital RF and algorithms for reliability of multi-level non-volatile memories. He received PhD in 2015 at Delft University of Technology about opto-mechatronics and adaptive optics for confocal microscopy. His main research interests are optical metrology, precision mechatronics systems, and biomedical imaging.

Georg Schitter is Professor for Advanced Mechatronic Systems at the Automation and Control Institute (ACIN) of TU Wien. He received an MSc in Electrical Engineering from TU Graz, Austria (2000) and an MSc and PhD degree from ETH Zurich, Switzerland (2004). His primary research interests are on high-performance mechatronic systems, particularly for applications in the hightech industry, scientific instrumentation, and mechatronic imaging systems, such as AFM, scanning laser and LIDAR systems, telescope systems, adaptive optics, and lithography systems for semiconductor industry. He received the journal best paper award of IEEE/ASME Transactions on Mechatronics (2017), of the IFAC Mechatronics (2008–2010), of the Asian Journal of Control (2004–2005), and the 2013 IFAC Mechatronics Young Researcher Award. He served as an Associate Editor for IFAC Mechatronics, Control Engineering Practice, and for the IEEE Transactions on Mechatronics.

Published version of the article: D. Brunner, H.W. Yoo, and G. Schitter, "Precise phase control of resonant MOEMS mirrors by comb-drive current feedback", *Mechatronics*, vol. 71, 102420, 2020. DOI: 10.1016/j.mechatronics.2020.102420